

The effect of ribosomal protein S15a in lung adenocarcinoma

Yifan Zhang, Guangxin Zhang, Xin Li, Bingjin Li, Xingyi Zhang

Background: RPS15A (ribosomal protein S15A) promotes mRNA/ribosome interactions in translation . It is critical for the process of eukaryotic protein biosynthesis. Recently, aberrantly expressed RPS15A was found in the virus hepatitis and malignant tumors. However, the role of RPS15A has not been fully revealed on the development of lung cancer. **Method:** In this study, a tissue microarray (TMA) of primary lung adenocarcinoma tissue specimens was carried out. Furthermore, to further investigate the function of RPS15A in lung cancer, RPS15A-specific short hairpin RNA (shRNA) expressing lentivirus (Lv-shRPS15A) was constructed and used to infect H1299 and A549 cells. **Result:** Our data showed that RPS15A expression was increase in tumor tissues. Furthermore, the knockdown of RSP15A inhibited cancer cell growth and induced apoptosis in the cancer cells. Gene expression profile microarray also revealed that the P53 signaling pathway was activated in Lv-shRPS15A-infected cancer cells. **Conclusion:** Taken together, our results demonstrate that RPS15A is a novel oncogene in non-small cell lung cancer and may be a potential therapeutic target in lung cancer.

1 **The effect of ribosomal protein S15a in lung adenocarcinoma**

2

3 Yifan Zhang¹, Guangxin Zhang¹, Xin Li², Bingjin Li^{2*} and Xingyi Zhang^{1*}

4 ¹ Department of Thoracic Surgery, the Second Hospital of Jilin University, Changchun, China
5 130041

6 ² Jilin provincial key laboratory on molecular and chemical genetic, the Second Hospital of Jilin
7 University, Changchun, China 130041

8

9

10

11

12 ***Corresponding author**

13 Xingyi Zhang,

14 Department of Thoracic Surgery

15 The Second Hospital of Jilin University

16 218 Ziqiang street Changchun China 130041

17 Email: xyzhang@jlu.edu.cn

18

19 Bingjin Li,

20 Jilin provincial key laboratory on molecular and chemical genetic

21 The Second Hospital of Jilin University

22 218 Ziqiang street Changchun China 130041

23 Email: bingjinli@hotmail.com

24 **Abstract**

25 **Background:** RPS15A (ribosomal protein S15A) promotes mRNA/ribosome interactions in
26 translation. It is critical for the process of eukaryotic protein biosynthesis. Recently, aberrantly
27 expressed RPS15A was found in the virus hepatitis and malignant tumors. However, the role of
28 RPS15A has not been fully revealed on the development of lung cancer.

29 **Method:** In this study, a tissue microarray (TMA) of primary lung adenocarcinoma tissue
30 specimens was carried out. Furthermore, to further investigate the function of RPS15A in lung
31 cancer, RPS15A-specific short hairpin RNA (shRNA) expressing lentivirus (Lv-shRPS15A) was
32 constructed and used to infect H1299 and A549 cells.

33 **Result:** Our data showed that RPS15A expression was increase in tumor tissues. Furthermore,
34 the knockdown of RSP15A inhibited cancer cell growth and induced apoptosis in the cancer cells.
35 Gene expression profile microarray also revealed that the P53 signaling pathway was activated in
36 Lv-shRPS15A-infected cancer cells.

37 **Conclusion:** Taken together, our results demonstrate that RPS15A is a novel oncogene in non-
38 small cell lung cancer and may be a potential therapeutic target in lung cancer.

40 Introduction

41

42 Lung cancer is the most prevalent malignant tumor and the leading cause of cancer-related death
43 in the world (Jemal et al. 2011). The principal histological forms of lung cancer have been well
44 established. Approximately 85% of lung cancer cases are non-small cell lung cancer (NSCLC).
45 Adenocarcinoma is the most commonly diagnosed type (Butnor & Beasley 2007). Despite
46 advances in surgical techniques and other therapeutic strategies, most patients diagnosed with
47 lung cancer ultimately succumb to this disease within 5 years (Miller 2005; Paleari et al. 2008).
48 Therefore, comprehensive understanding of the molecular mechanisms underlying lung cancer
49 progress is important for the development of optimal anti-cancer therapy (Hensing et al. 2014).

50

51 Tumorigenesis involves multistep development to acquire certain malignant capabilities, such as,
52 sustaining proliferative signaling, resisting cell apoptosis, activating invasion and metastasis et al
53 (Hanahan & Weinberg 2011). Underlying these abilities of tumor cells, rapid *de novo*
54 biosynthesis of functional ribosome is essential for cancer cells to aggressively grow and obtain
55 multiple malignant phenotypes. Ribosomes are composed of diverse ribosomal RNAs in
56 eukaryotic organs. So far, most ribosomal proteins have been identified to bind to certain regions
57 of ribosomal RNA and perform catalytic functions. Many ribosomal proteins have various extra-
58 ribosomal functions, such as DNA repair, transformation, development, apoptosis, and
59 transcription (Lee et al. 2010; Nishiura et al. 2013; Nosrati et al. 2014). Some studies show that
60 these proteins may play a role in human tumor development and progression. For example,
61 depletion of ribosomal protein L26 and L29 suppress the proliferation of human pancreatic
62 cancer PANC-1 cells (Li et al. 2012), while RPL22 expression is highly associated with NSCLC
63 (Yang et al. 2013).

64

65 Human ribosomal protein S15a (RPS15A) is a highly conserved cellular gene that maps to
66 human chromosome 16p12.3 locus (Chan et al. 1994; Schaap et al. 1995). It promotes
67 mRNA/ribosome binding in translation via the interactions with the cap-binding subunit of
68 eukaryotic initiation factor 4F (eIF-4F) (Linder & Prat 1990). In yeast, G1/S cell cycle phase
69 arrest induced by *cdc33* (encoding eIF-4F in yeast) mutation could be reversed by RPS15A over-
70 expression, these findings suggest that RPS15A may play a role in cell cycle transition (Lavoie et
71 al. 1994). RPS15A over-expression also facilitates hepatocellular growth via promoting cell
72 cycle transition and accelerates tumor formation *in vitro* (Lian et al. 2004), whereas RPS15A
73 mRNA down-regulation inhibited hepatic cancer cell growth (Xu et al. 2014). However, the role
74 of RPS15A in lung cancer has not been completely studied.

75

76 The present study was aimed to investigate whether RPS15A is involved in the development and

77 progression of lung cancer. A tissue microarray was carried out to determine the expression of
78 RPS15A. To examine its functional role in lung cancer progress, an RPS15A-specific small
79 interfering RNA (siRNA)-lentiviral vector was constructed to block RPS15A expression in
80 human lung adenocarcinoma H1299 and A549 cells. Furthermore, the impacts of RPS15A
81 silencing on the growth of the cancer cells were examined by MTT assay and colony formation
82 assay. In addition, the effects of RPS15A knockdown on the apoptosis of H1299 and A549 cells
83 were determined by flow cytometry analysis. To further explore the potential molecular
84 mechanisms, we also performed a human whole genome oligo microarray followed by a KEGG
85 pathway enrichment analysis.

86

88 **Materials and methods**

89

90 **Tissue microarray and immunohistochemical staining**

91

92 Tumor samples were collected from 75 patients with lung adenocarcinoma at the Department of
93 Thoracic Surgery, The Second Affiliated Hospital of Jilin University, China, from July 2005 to
94 December 2011. All the tissue samples were obtained from surgery with informed consent and
95 with institutional review board approval of the hospital. Non-tumor samples from the
96 macroscopic tumor margin were isolated at the same time and used as the matched adjacent non-
97 neoplastic tissues. Expression of RPS15A protein was detected using immunohistochemical
98 analysis on commercially available tissue microarrays (TMAs) from Shanghai Zhuoli
99 Biotechnology Co., Ltd. (Shanghai, China), which contained a total of 150 tissue samples of
100 tumor or adjacent normal tissues from 75 patients. There were 44 male patients and 31 female
101 patients aging from 32 to 80 years, with an average age of 58 years old. The tumors were
102 classified according to the tumor nodes metastasis (TNM) stage revised by the International
103 Union Against Cancer in 2002.

104

105 **Immunohistochemical staining and scoring**

106

107 To detect RPS15A expression in lung cancer, archival paraffin-embedded tumor samples were
108 used to build up tissue microarray (TMA) blocks for immunohistochemical (IHC) staining.
109 Immunohistochemical staining was performed using the Vectastain Elite ABC Kit (Vector
110 Laboratories, Burlingame, CA) according to the manufacturer's protocol. Briefly, TMA sections
111 were deparaffinized and hydrated in xylene, ethanol and water. After heat-induced antigen
112 retrieval procedures, sections were incubated overnight at 4 °C with anti-RPS15A primary
113 antibody (1:50 dilution; Abcam). After the primary antibody was washed off, the ABC detection
114 system was performed by using biotinylated anti-rabbit IgG. The slides were counterstained with
115 haematoxylin and mounted in xylene mounting medium for examination. Negative controls were
116 treated identically but with the primary antibody omitted. Three researchers evaluated
117 immunoreactivity independently. The percentage of positive tumor cells was determined by each
118 observer, and the average of three scores was calculated. The proportion of immunopositive cells
119 were categorized as following: intensity of staining: none (0), mild (1), moderate (2), strong (3);
120 percentage of the positive staining: 0 (-), <15 % (+), 15–50 % (++), >50 % (+++). To obtain final
121 statistical results, - and + groups were considered as negative.

122

123 **Cell lines**

124

125 Lung adenocarcinoma cell lines H1299 and A549, lung squamous cancer cell line SK-MES-1, as
126 well as small cell lung cancer cell line H1688 (Cell Bank of Chinese Academy of Sciences,
127 Shanghai, China) and human embryonic kidney (HEK) 293T cell line (American Type Culture
128 Collection, ATCC, Manassas, VA, USA) were maintained in DMEM (Hyclone, Logan, UT,
129 USA) with 10% FBS (Hyclone) and penicillin/streptomycin at 37°C in humidified atmosphere of
130 5% CO₂.

131

132 **Construction and infection of RPS15A short hairpin (shRNA)-expressing lentivirus**

133

134 To permit robust inducible RNAi-mediated RPS15A silencing in tumor cells, RPS15A-specific
135 shRNA containing lentiviral vector was constructed. The RNAi was designed based on
136 conservative cDNA fragments within the coding region of human RPS15A gene (NM_001019)-
137 targeting sequence (5'-GCAACTCAAAGACCTGGAA -3') of oligo nucleotides. The sequences
138 were annealed and ligated into the Age I/EcoR I (NEB, Ipswich, MA, USA)-linearized pGCSIL-
139 GFP vector (Shanghai Genechem Co. LTD., Shanghai, China). The lentiviral-based shRNA-
140 expressing vectors were confirmed by DNA sequencing. Recombinant lentiviral vectors and
141 packaging vectors were then cotransfected into 293T cells using Lipofectamine 2000 (Invitrogen,
142 Carlsbad, CA, USA), according to the manufacturer's instructions for the generation of
143 recombinant lentiviruses Lv-shRPS15A and negative control Lv-shCon. The culture supernatants
144 containing lentiviral particles expressing Lv-shRPS15A and Lv-shCon were harvested and ultra-
145 centrifuged 48 h after transfection, respectively. H1299 and A549 cells were infected with the
146 lentiviruses at multiplicity of infection (MOI) of 10 and 20, respectively.

147

148 **Quantitative real-time PCR analysis**

149

150 In brief, total RNA was extracted using TRIzol reagent (Invitrogen, Carlsbad, CA). The reverse
151 transcription reactions were carried out following the protocol of the M-MLV Reverse
152 Transcriptase (Promega Corp., Madison, WI). Real-time quantitative PCR analysis was
153 performed using SYBR Master Mixture Kit (TaKaRa, Dalian, China). The primer sequences for
154 PCR amplification of RPS15A were 5'-CTCCAAAGTCATCGTCCGGTT-3' and 5'-
155 TGAGTTGCACGTCAAATCTGG-3'. GAPDH was applied as an internal control. The primer
156 sequences of GAPDH were 5'-TGA CTTCAACAGCGACACCCA-3' and 5'-
157 CACCCTGTTGCTGTAGCCAAA-3'. $2^{-\Delta\Delta CT}$ method was adopted to calculate the relative
158 expression levels of RPS15A by subtracting CT values of the control gene from the CT values of
159 RPS15A.

160

161 **MTT proliferation and colony formation assay**

162

163 Briefly, exponentially growing cancer cells were inoculated into 96-well plates with 2×10^4 cells
164 per well. After incubation for 24, 48, 72, 96 and 120 h, 10 μ l of sterile MTT (5 mg/ml) was
165 added into each well. Following incubation at 37°C for 4 h, the reaction was blocked by adding
166 100 μ l of dimethyl sulfoxide. The formazan production was determined by measurement of the
167 spectrometric absorbance at 490 nm. The values obtained are proportional to the amount of
168 viable cells and each experiment was repeated three times. In colony formation assay, H1299 and
169 A549 cells infected with Lv-shRPS15A or Lv-shCon were seeded in six-well plates with 5×10^2
170 cells per well and cultured at 37°C with 5% CO₂ for 14 days. The cell colonies were washed
171 twice with PBS, fixed in 4% paraformaldehyde for 30 min and stained with Giemsa for 20 min.
172 Individual colonies with more than 50 cells were counted under a fluorescence microscope.

173

174 **Apoptosis assay by fluorescence-activated cell sorting (FACS) analysis**

175

176 In apoptotic cell detection, exponentially growing H1299 and A549 cells were seeded in six-well
177 plates. After 48 h, cells were collected and washed with pre-chilled PBS (4°C). Then, the cells
178 were centrifuged at 1500 rpm for 5 min. After discarding the supernatant, the pellet was
179 resuspended with binding buffer. The cells were then incubated with 5 μ l Annexin V-APC for 15
180 min in the dark. After filtration of the cell suspension, the analysis of apoptotic cells was
181 performed by FACS can (Becton– Dickinson).

182

183 **Gene expression profile microarray**

184

185 Briefly, A549 cells were seeded in a six-well plate at a density of 4×10^5 cells per well and
186 infected by Lv-shRPS15A and Lv-shCon at MOI of 20, respectively. After 96h, the total RNAs
187 were extracted using TRIzol reagent (Invitrogen, Carlsbad, CA) and were used for cDNA
188 synthesis and labeling, microarray hybridization and then followed by flour-labeled cDNA
189 hybridizing their complements on the chip (Affymetrix, Santa Clara, CA, USA). The resulting
190 localized concentrations of fluorescent molecules were detected and quantified by GeneChip
191 Scanner 3000 (Affymetrix). Finally, the data were analyzed by Expression Console Software
192 (Affymetrix) with default RMA parameters. Data are representative of three separate assays.

193

194 **Gene ontology annotation and KEGG pathway enrichment analysis**

195

196 The gene ontology analysis was performed to functionally annotate the differentially expressed
197 genes according to the Gene Ontology database (<http://www.geneontology.org/>). The pathway
198 enrichment analysis was performed according to the KEGG (Kyoto Encyclopedia of Genes and

199 Genomes) database. The Fisher's exact test and χ^2 test were applied to classify the significant GO
200 categories and pathways, and the FDR was calculated to correct the *P*-value by multiple
201 comparison tests. A *P*-value <0.05 and an FDR <0.05 were set as thresholds to select significant
202 GO categories and pathways.

203

204 **Western Blotting assay**

205

206 In brief, A549 cells were collected and lysed with precooled lysis buffer after 96 h of infection.
207 Total protein was extracted from the cells and determined by the BCA method. Protein (20 μ g)
208 was loaded onto a 10% SDS-PAGE gel. The gel was run at 30 mA for 2 h and transferred to
209 poly-vinylidene difluoride membrane (Millipore, Billerica, MA, USA). The resulting membrane
210 was blocked in 5% non-fat dry milk blocking buffer and then probed with rabbit anti-P21
211 (1:2,000 dilution; Abcam, Cambridge, MA; Cat. ab7960), mouse anti-TP53I3 (1:500 dilution;
212 Abcam, Cambridge, MA; Cat. ab123917), rabbit anti-SESN2 (1:500 dilution; Abcam,
213 Cambridge, MA; Cat. ab57810) and mouse anti-GAPDH (1:6,000; Santa Cruz Biotechnology,
214 Inc., Santa Cruz, CA) overnight at 4 °C. The protein level of GAPDH was used as a control and
215 detected by an anti-GAPDH antibody. The membrane was washed three times with Tris-buffered
216 saline Tween-20 (TBST), followed by incubation for 2 h with anti-rabbit and anti-mouse IgG at a
217 1:5,000 dilution (Santa Cruz Biotechnology, Inc.). The membrane was developed using
218 enhanced chemiluminescence (Amersham, UK). Bands on the developed films were quantified
219 with an ImageQuant densitometric scanner (Molecular Dynamics, Sunny-Vale, CA, USA).

220

221 **Statistic analysis**

222 Data were expressed as mean \pm SD. Comparisons were performed by two-sided independent
223 Student's test, one-way ANOVA analysis and χ^2 test using SPSS software for Windows version
224 23.0 (SPSS, Chicago, USA). Kaplan-Meier survival curves were plotted and log rank test was
225 done. Statistical significance was accepted when *P*<0.05. All experiments carried out in this
226 study were repeated three independent times.

227 Result

228

229 RPS15A was significantly overexpressed in lung adenocarcinoma tissues

230

231 We detected the expression of RPS15A protein in a tissue microarray (TMA) of primary lung
232 adenocarcinoma and adjacent normal lung tissue specimens using immunohistochemical staining
233 with an anti-RPS15A antibody. RPS15A immunostaining was primarily detected in cytoplasm.
234 Representative examples of RPS15A protein expression in lung cancer and normal lung samples
235 are shown in Fig. 1a. The immunopositive rates of RPS15A in lung adenocarcinoma and normal
236 lung tissues were 66.7% (50/75) and 42.7% (32/75), indicating that RPS15A was highly
237 expressed in lung cancer in comparison with adjacent normal tissues, as shown in Table.1
238 ($P<0.001$). The correlation between RPS15A expression and different clinical pathological
239 factors in lung adenocarcinoma is shown in Table 2. No significant correlation was found
240 between RPS15A expression and age, grade, TNM stage, tumor size and lymph node metastasis
241 ($P<0.05$). Kaplan-Meier survival analysis of overall prognosis between patients with higher
242 RPS15A expression and patients with low RPS15A expression was carried out. No significant
243 correlation between RPS15A expression and overall prognosis was found, as shown in Fig 1b.

244

245 Efficacy of lentivirus-mediated RNAi targeting RPS15A

246

247 Quantitative real-time PCR was performed to detect the fundamental expression of RPS15
248 mRNA in several lung cancer cell lines, including lung adenocarcinoma cell lines H1299, A549
249 and lung squamous cancer cell line SK-MES-1, as well as small cell lung cancer cell line H1688.
250 As shown in Fig. 2a, RPS15A expression levels were quite obvious in the cancer cell lines.
251 Consequently, loss of function assay was applied through RPS15A knockdown. H1299 and
252 A549 cell lines were selected for subsequent studies. To knockdown RPS15A expression, H1299
253 and A549 cells were infected by the lentiviruses stably expressing RPS15A-specific shRNA (Lv-
254 shRPS15A). Lentivirus expressing negative shRNA (Lv-shCon) was used as negative control.
255 More than 80% of GFP-expressing cells were observed under fluorescence microscope after 72 h
256 (Fig. 2b). The silencing effect of lentivirus mediated RPS15A RNAi on RPS15A expression in
257 H1299 and A549 cells was examined through real-time PCR and Western Blotting assay. The
258 expression level of RPS15A in the Lv-shRPS15A infected cells was significantly lower than that
259 in the Lv-shCon infected cells (Fig. 2c, 2d). Therefore, these data indicated the high efficacy of
260 lentivirus mediated RPS15A silence in lung cancer cells.

261

262 RPS15A silence inhibited NSCLC cell growth *in vitro*

263

264 To investigate the role of RPS15A in the proliferation of lung cancer cells, the proliferative
265 abilities of Lv-shCon and Lv-shRPS15A infected H1299 and A549 cells was determined by
266 MTT assay. During the 120 hour incubation period, the growth of Lv-shRPS15A infected cells
267 was significantly slower than that of Lv-shCon infected cells at the time points of 48 h, 72 h, 96
268 h and 120 h (Fig. 3a and 3b). To investigate the effect of RPS15A downregulation on tumor
269 formation, colony formation assay was performed. Quantitative analysis of colonies showed that
270 after incubation for 10 days, the number of colonies in Lv-shRPS15A infected cells was
271 significantly lower than that in the Lv-shCon infected cells (Fig. 3c, 3d, 3e and 3f). Therefore,
272 the low colony-forming efficiency of Lv-shRPS15A infected H1299 and A549 cells
273 demonstrated that RPS15A silencing inhibited the colony forming ability of lung cancer cells *in*
274 *vitro*.

275

276 **RPS15A silence triggered cell apoptosis *in vitro***

277

278 To determine whether RPS15A knockdown induces apoptosis in H1299 and A549 cells,
279 Annexin V-APC staining was performed and the percentage of apoptotic cells was detected by
280 flow cytometry. As shown in Fig. 4a, 4b, 4c and 4d, Lv-shRPS15A infected cells exhibited
281 significantly higher proportion of apoptotic cells than that of Lv-shCon infected cells, especially
282 in Lv-shRPS15A infected A549 cells. This suggested that downregulation of RPS15A expression
283 might trigger apoptosis in lung cancer cells, which contributed to the cell growth suppression.

284

285 **RPS15A knockdown activated P53 signaling pathway *in vitro***

286

287 To explore the potential downstream mechanisms underlying the actions of RPS15A silencing, a
288 cDNA microarray assay was performed to compare the differential gene expression profiles
289 between Lv-shRPS15A infected and Lv-shCON infected A549 cancer cells. Microarray analysis
290 demonstrated that 885 genes were upregulated and 566 genes were downregulated significantly
291 in Lv-shRPS15A infected cancer cells when compared to Lv-shCON infected cells. To further
292 classify the function of these genes, GO analysis was carried out. The most significant GO
293 categories of biological processes included protein, biopolymer and cellular macromolecule
294 metabolic processes. Of these genes, the most enriched GO in terms of molecular function
295 involved DNA binding, cation and ion binding and enzyme regulator activity. KEGG pathway
296 enrichment analysis revealed that certain signaling pathways participated in the tumor inhibition
297 induced by RPS15A knockdown, of which P53 signaling pathway members were most evidently
298 annotated. The top 20 significantly perturbed pathways are listed in Table 3. To confirm the P53
299 pathway activation, the expressions of key factors of P53 signaling pathway were determined

300 through western blotting. Consistent with microarray results, P21 and TP53I3 expressions were
301 upregulated by RPS15A knockdown, while SESN2 expression was downregulated, as shown in
302 Fig.4e.
303

305 Discussion

306

307 Therapeutic drugs targeting cancer-related molecules can specifically inhibit malignant cells,
308 causing minimal adverse off target reactions because of the well-defined mechanisms (Chen et al.
309 2013). Therefore, identification of molecular factors responsible for pulmonary carcinogenesis
310 and elucidation of their underlying mechanisms of proliferation are urgently needed for novel
311 therapeutic targets.

312

313 Earlier genetic studies in zebrafish suggested that many ribosomal protein genes are haploid-
314 sufficient suppressor gene that are highly related to tumorigenesis (Amsterdam et al. 2004).
315 Ribosomal proteins are abundant in most cells and well known for their functional role in the
316 assembly of ribosomal subunits at the early stages of translation. In addition, ribosomal proteins
317 have been found to regulate cell proliferation, apoptosis, DNA repair and gene transcription.
318 Currently, ribosomal proteins are emerging as novel regulators of cancer cell growth, whose
319 mutations and changes of expression level are highly relevant to human malignancies. RPS15A,
320 as a component of the 40S ribosomal subunit, has been found to facilitate the binding of capped
321 mRNA to the ribosomal subunit 40S in translation initiation. Furthermore, it has been reported
322 that downregulation of its mRNA expression in hepatocellular carcinoma cells significantly
323 inhibits tumor growth, suggesting that RPS15A may play a role in human carcinogenesis. Yet,
324 up to now, little is known about its function in NSCLC cells.

325

326 To determine the expression levels of RPS15A in lung adenocarcinoma tissues, TMAs was
327 performed and revealed that RPS15A was highly expressed in lung cancer tissue. Therefore, we
328 hypothesized that RPS15A may play an important role in the proliferation of lung cancer. In this
329 regard, a lentivirus-mediated RNAi system was applied to inhibit RPS15A mRNA expression in
330 human lung adenocarcinoma H1299 and A549 cells *in vitro*. Lentivirus expressing RPS15A-
331 specific shRNA was constructed and used to infect H1299 and A549 cells. The efficiency of
332 lentivirus-induced silencing of endogenous RPS15A was confirmed by qPCR and western
333 blotting assay. To determine the impact of RPS15A knockdown on the lung cancer growth *in*
334 *vitro*, an MTT assay and colony formation assay were carried out. As a result, downregulation of
335 RPS15A expression greatly impaired the proliferation and colony-forming ability of H1299 and
336 A549 cells. Furthermore, flow cytometry analysis data showed that RPS15A silencing induced
337 apoptosis as characterized by the prominent presence of apoptotic cancer cells.

338

339 To elucidate the downstream mechanisms underlying RPS15A silence in lung cancer, we carried
340 out a human whole genome oligo microarray and KEGG pathway enrichment analysis. The data
341 revealed that the P53 signaling pathway was activated significantly in Lv-shRPS15A infected

342 A549 cells. The P53 pathway has been well known for its anticancer function through initiating
343 apoptosis, cell cycle arrest, maintaining genomic stability, angiogenesis inhibition etc (Levine &
344 Oren 2009). To confirm the P53 signaling activation, we determined the expression of P21,
345 TP53I3 and SESN2 by using western blotting. P21(P21), which is tightly controlled by the tumor
346 suppressor protein p53, is a potent cyclin-dependent kinase inhibitor that binds to cyclin-CDK2
347 or -CDK4 complexes, thus functioning as a regulator of cell cycle progression at G1 (el-Deiry et
348 al. 1993).TP53I3 is induced by the tumor suppressor p53 and is thought to be involved in p53-
349 mediated cell death (Polyak et al. 1997). SESN2 is also known for its function in the regulation
350 of cell growth and survival in cellular response to different stress conditions (Hay 2008).

351

352 Ribosomal proteins are often classified as cell growth associated molecules due to their key role
353 in protein synthesis (Eid et al. 2014; Lian et al. 2004; Wang et al. 2014). Our finding that
354 RPS15A downregulation inhibits NSCLC cell growth is also supported by previous studies that
355 RPS15A knockdown also inhibits hepatic cancer cell growth (Xu et al. 2014). Like other
356 ribosomal proteins, RPS15A has been found to involve extra-ribosomal functions in cell growth,
357 apoptosis and cell cycle transition. In this study, our findings that RPS15A induced apoptosis and
358 cell cycle phase arrest in lung cancer A549 cells further supported that P53 signaling is critical
359 for the regulation of apoptosis and cell cycle transition. However, to date, the issue of whether
360 and how RPS15A interacts with other regulators remains poorly studied, and further
361 investigation is warranted to elucidate the detailed mechanisms underlying the action of RPS15A.
362 Taken together, our study demonstrated that RPS15A might serve as an upstream modulator of
363 P53 signaling pathway.

364

365 In conclusion, RPS15A expression was increased in tumor tissues. Furthermore, the knockdown
366 of RSP15A inhibited cancer cell growth and induced apoptosis in the cancer cells. Gene
367 expression profile microarray also revealed that the P53 signaling pathway was activated in Lv-
368 shRPS15A-infected cancer cells. Therefore, our findings demonstrate that RPS15A is a novel
369 oncogene in non-small cell lung cancer and may be a potential therapeutic target in lung cancer.

370

371 **References**

372

373 Amsterdam A, Sadler KC, Lai K, Farrington S, Bronson RT, Lees JA, and Hopkins N. 2004. Many ribosomal protein
374 genes are cancer genes in zebrafish. *PLoS Biol* 2:E139.

375 Butnor KJ, and Beasley MB. 2007. Resolving dilemmas in lung cancer staging and histologic typing. *Arch Pathol Lab*
376 *Med* 131:1014-1015.

377 Chan YL, Olvera J, Paz V, and Wool IG. 1994. The primary structure of rat ribosomal protein S15a. *Biochem Biophys*
378 *Res Commun* 200:1498-1504.

379 Chen X, Liu Y, Roe OD, Qian Y, Guo R, Zhu L, Yin Y, and Shu Y. 2013. Gefitinib or erlotinib as maintenance therapy in
380 patients with advanced stage non-small cell lung cancer: a systematic review. *PLoS One* 8:e59314.

381 Eid R, Sheibani S, Gharib N, Lapointe JF, Horowitz A, Vali H, Mandato CA, and Greenwood MT. 2014. Human

382 ribosomal protein L9 is a Bax suppressor that promotes cell survival in yeast. *FEMS Yeast Res* 14:495-507.
383 el-Deiry WS, Tokino T, Velculescu VE, Levy DB, Parsons R, Trent JM, Lin D, Mercer WE, Kinzler KW, and Vogelstein B.
384 1993. WAF1, a potential mediator of p53 tumor suppression. *Cell* 75:817-825.
385 Hanahan D, and Weinberg RA. 2011. Hallmarks of cancer: the next generation. *Cell* 144:646-674.
386 Hay N. 2008. p53 strikes mTORC1 by employing sestrins. *Cell Metab* 8:184-185.
387 Hensing T, Chawla A, Batra R, and Salgia R. 2014. A personalized treatment for lung cancer: molecular pathways,
388 targeted therapies, and genomic characterization. *Adv Exp Med Biol* 799:85-117.
389 Jemal A, Bray F, Center MM, Ferlay J, Ward E, and Forman D. 2011. Global cancer statistics. *CA Cancer J Clin* 61:69-
390 90.
391 Lavoie C, Tam R, Clark M, Lee H, Sonenberg N, and Lasko P. 1994. Suppression of a temperature-sensitive cdc33
392 mutation of yeast by a multicopy plasmid expressing a Drosophila ribosomal protein. *J Biol Chem*
393 269:14625-14630.
394 Lee SB, Kwon IS, Park J, Lee KH, Ahn Y, Lee C, Kim J, Choi SY, Cho SW, and Ahn JY. 2010. Ribosomal protein S3, a
395 new substrate of Akt, serves as a signal mediator between neuronal apoptosis and DNA repair. *J Biol*
396 *Chem* 285:29457-29468.
397 Levine AJ, and Oren M. 2009. The first 30 years of p53: growing ever more complex. *Nat Rev Cancer* 9:749-758.
398 Li C, Ge M, Yin Y, Luo M, and Chen D. 2012. Silencing expression of ribosomal protein L26 and L29 by RNA
399 interfering inhibits proliferation of human pancreatic cancer PANC-1 cells. *Mol Cell Biochem* 370:127-139.
400 Lian Z, Liu J, Li L, Li X, Tufan NL, Wu MC, Wang HY, Arbutnot P, Kew M, and Feitelson MA. 2004. Human S15a
401 expression is upregulated by hepatitis B virus X protein. *Mol Carcinog* 40:34-46.
402 Linder P, and Prat A. 1990. Baker's yeast, the new work horse in protein synthesis studies: analyzing eukaryotic
403 translation initiation. *Bioessays* 12:519-526.
404 Miller YE. 2005. Pathogenesis of lung cancer: 100 year report. *Am J Respir Cell Mol Biol* 33:216-223.
405 Nishiura H, Zhao R, Chen J, Taniguchi K, and Yamamoto T. 2013. Involvement of regional neutrophil apoptosis
406 promotion by ribosomal protein S19 oligomers in resolution of experimental acute inflammation. *Pathol*
407 *Int* 63:581-590.
408 Nosrati N, Kapoor NR, and Kumar V. 2014. Combinatorial action of transcription factors orchestrates cell cycle-
409 dependent expression of the ribosomal protein genes and ribosome biogenesis. *FEBS J*.
410 Paleari L, Russo P, Cesario A, and Granone P. 2008. Factors predicting poor survival after resection of stage IA non-
411 small cell lung cancer. *J Thorac Cardiovasc Surg* 136:241-242.
412 Polyak K, Xia Y, Zweier JL, Kinzler KW, and Vogelstein B. 1997. A model for p53-induced apoptosis. *Nature* 389:300-
413 305.
414 Schaap PJ, de Groot PW, Muller Y, van Griensven LJ, and Visser J. 1995. Molecular cloning and sequence of the
415 cytoplasmic ribosomal protein S15a gene from *Agaricus bisporus*. *Exp Mycol* 19:160-162.
416 Wang L, Luo J, Nian Q, Xiao Q, Yang Z, and Liu L. 2014. Ribosomal protein S14 silencing inhibits growth of acute
417 myeloid leukemia transformed from myelodysplastic syndromes via activating p53. *Hematology* 19:225-
418 231.
419 Xu M, Wang Y, Chen L, Pan B, Chen F, Fang Y, Yu Z, and Chen G. 2014. Down-regulation of ribosomal protein S15A
420 mRNA with a short hairpin RNA inhibits human hepatic cancer cell growth in vitro. *Gene* 536:84-89.
421 Yang M, Sun H, Wang H, Zhang S, Yu X, and Zhang L. 2013. Down-regulation of ribosomal protein L22 in non-small
422 cell lung cancer. *Med Oncol* 30:646.
423

425 **Figure Legend**

426

427 **Figure 1.** Immunostaining of RPS15A in lung adenocarcinoma and adjacent normal tissues with
428 tissue microarray. (a) Three representative cases with different expression status of RPS15A,
429 ranging from negative, mild and strong expression were taken at 100× and 400× magnification
430 in lung cancer and normal tissues. (b) Kaplan-Meier survival analysis of overall prognosis
431 between patients with higher RPS15A expression and patients with low RPS15A expression.
432 Log-rank test was used to statistically calculate the difference.

433

434 **Figure 2.** Lentiviral mediated RPS15A downregulation. (a) Relative RPS15A mRNA level in
435 lung cancer cell lines (H1299, A549, SK-MES-1, H1688 and H1975). (b) Fluorescence
436 photomicrographs of H1299 and A549 cells 72h after lentivirus infection. (c, d) RPS15A mRNA
437 and protein expressions were dramatically downregulated in Lv-shRPS15A infected cells
438 evidenced by real-time PCR and Western blotting assay. **P<0.01 versus Lv-shCon.

439

440 **Figure 3.** The proliferation of H1299 and A549 cells was inhibited after Lv-shRPS15A infection
441 determined by MTT assay. (a, b). The colony formation abilities of H1299 and A549 cells were
442 determined by colony formation assay after Lv-shRPS15A infection. (c, d) Images of colonies
443 and statistical analysis of the number of colonies. (e, f) Images of colonies recorded under
444 microscope. *P<0.05, **P<0.01 versus Lv-shCon.

445

446 **Figure 4.** RPS15A knockdown induced apoptotic cells were determined by flow cytometry
447 analysis after Annexin V-APC staining. (a, b) Histograms of FACS analysis. (c, d) Percentage of
448 apoptotic cells. **P<0.01 versus Lv-shCon. (e) Key factors of P53 signaling pathway, such as
449 P21, TP53I3 and SESN2, were examined in Lv-shRPS15A infected A549 cells by using western
450 blotting method. The protein level of GAPDH was employed as a control.

451

452 **Table 1.** RPS15A expression in 75 lung adenocarcinoma and adjacent normal tissue specimens

453

454 **Table 2.** Correlation between RPS15A expression and clinicopathological factors in 75 lung
455 adenocarcinoma patients specimens.

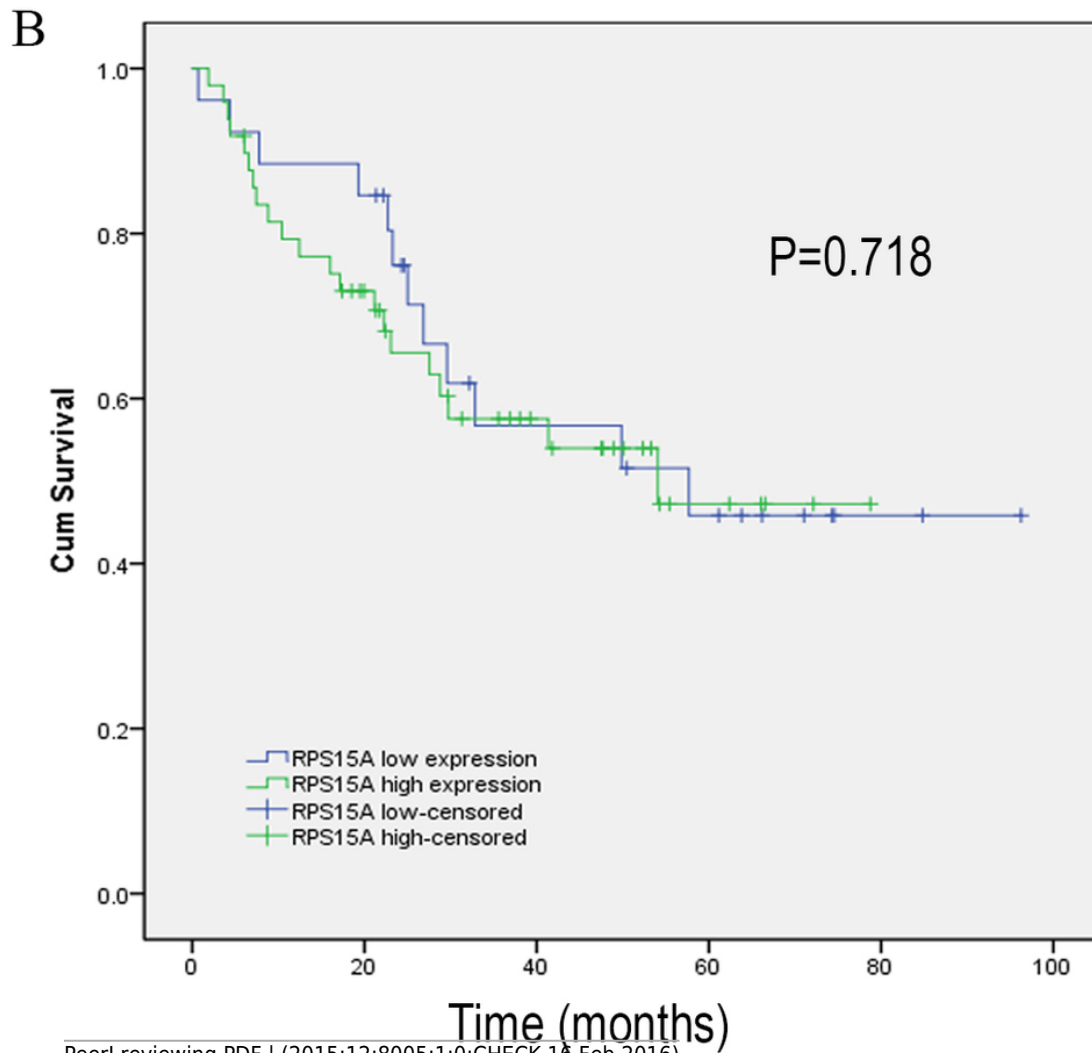
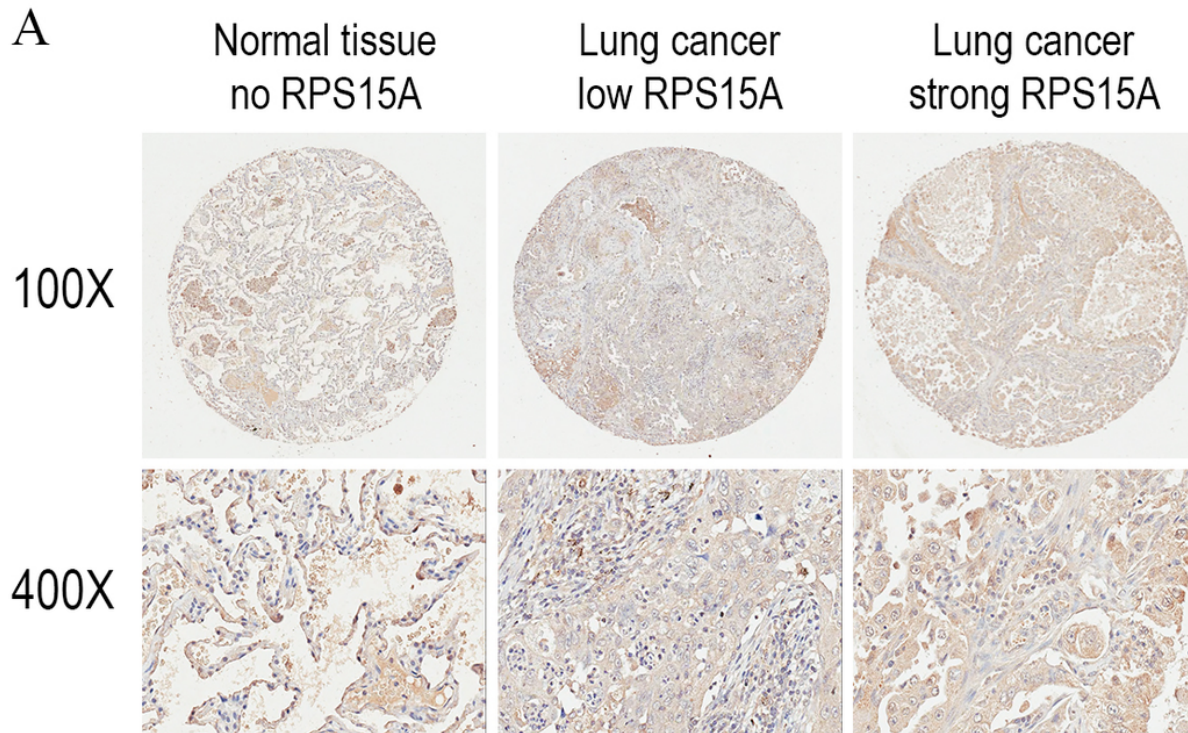
456

457 **Table 3.** KEGG pathway enrichment analysis revealed that P53 signaling pathway members
458 were most evidently annotated. Top 20 significantly perturbed pathways are listed.

1

Immunostaining of RPS15A with tissue microarray

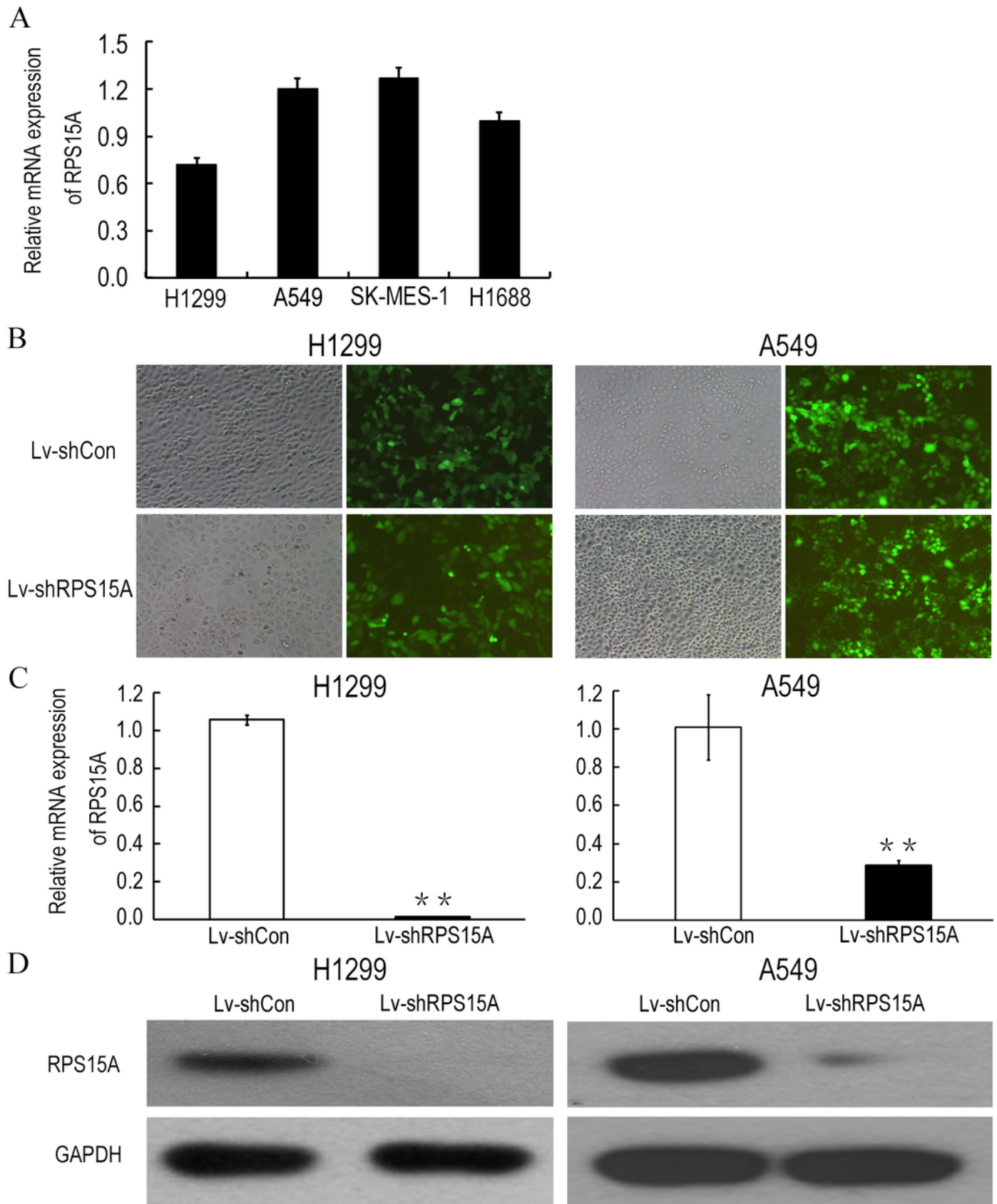
Immunostaining of RPS15A in lung adenocarcinoma and adjacent normal tissues with tissue microarray. (a) Three representative cases with different expression status of RPS15A, ranging from negative, mild and strong expression were taken at 100 × and 400 × magnification in lung cancer and normal tissues. (b) Kaplan-Meier survival analysis of overall prognosis between patients with higher RPS15A expression and patients with low RPS15A expression. Log-rank test was used to statistically calculate the difference.



2

Lentiviral mediated RPS15A downregulation.

Lentiviral mediated RPS15A downregulation. (a) Relative RPS15A mRNA level in lung cancer cell lines (H1299, A549, SK-MES-1, H1688 and H1975). (b) Fluorescence photomicrographs of H1299 and A549 cells 72h after lentivirus infection. (c, d) RPS15A mRNA and protein expressions were dramatically downregulated in Lv-shRPS15A infected cells evidenced by real-time PCR and Western blotting assay. ** $P < 0.01$ versus Lv-shCon.



3

The proliferation of H1299 and A549 cells

The proliferation of H1299 and A549 cells was inhibited after Lv-shRPS15A infection determined by MTT assay. (a, b). The colony formation abilities of H1299 and A549 cells were determined by colony formation assay after Lv-shRPS15A infection. (c, d) Images of colonies and statistical analysis of the number of colonies. (e, f) Images of colonies recorded under microscope. * $P < 0.05$, ** $P < 0.01$ versus Lv-shCon.

4

RPS15A knockdown induced apoptotic cells

RPS15A knockdown induced apoptotic cells were determined by flow cytometry analysis after Annexin V-APC staining. (a, b) Histograms of FACS analysis. (c, d) Percentage of apoptotic cells. $**P < 0.01$ versus Lv-shCon. (e) Key factors of P53 signaling pathway, such as P21, TP53, and SESN2, were examined in Lv-shRPS15A infected A549 cells by using western blotting method. The protein level of GAPDH was employed as a control.

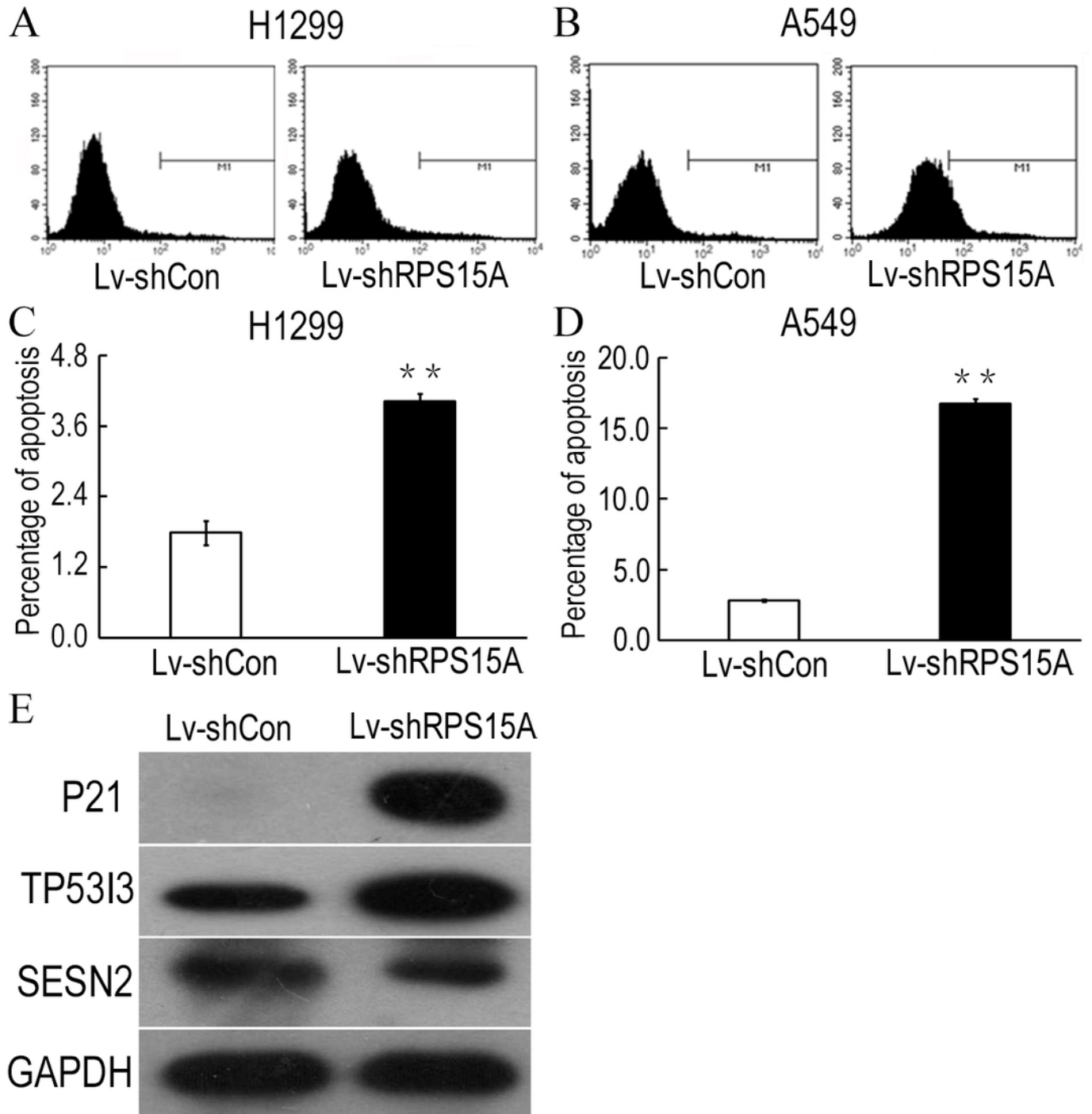


Table 1 (on next page)

RPS15A expression in 75 lung adenocarcinoma and adjacent normal tissue specimens .

- 1 **Table 1** RPS15A expression in 75 lung adenocarcinoma and adjacent normal tissue specimens
- 2 *P values were obtained with the χ^2 test, P<0.001.

Histological types	Number	RPS15A expression				p*
		-	+	++	+++	
Cancer	75	11	19	15	35	0.000
Normal tissue	75	5	38	26	6	

Table 2 (on next page)

Correlation between RPS15A expression and clinicopathological factors in 75 lung adenocarcinoma patients specimens.

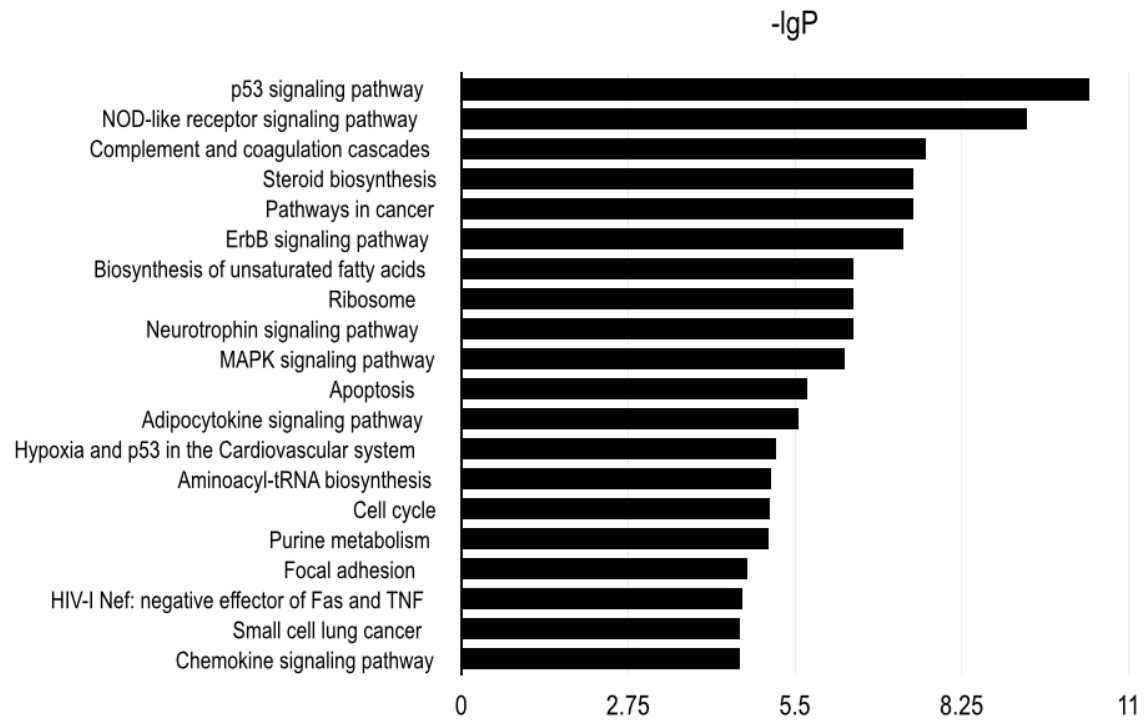
1 **Table 2** Correlation between RPS15A expression and clinicopathological factors in 75 lung
 2 adenocarcinoma tissue specimens

Variables	All patients	RPS15A expression		p*
		Negative	Positive	
Total	75	26	49	
Age(y)				
≤60	48	14	25	1.000
>60	27	12	24	
Gender				
Male	43	19	24	0.053
Female	32	7	25	
TNM stage				
I~II	47	20	36	0.788
III~IV	28	6	13	
Tumor size				
≤3cm	8	1	7	0.249
>3cm	67	25	42	
Lymph node metastasis				
Yes	28	8	20	0.458
No	47	18	29	

3 *P values were obtained with the χ^2 test

Table 3 (on next page)

KEGG pathway enrichment analysis revealed that P53 signaling pathway members were most evidently annotated. Top 20 significantly perturbed pathways are listed.

1 **Table 3** Top 20 highly expressed signaling pathways induced by RPS15A silencing

2

3